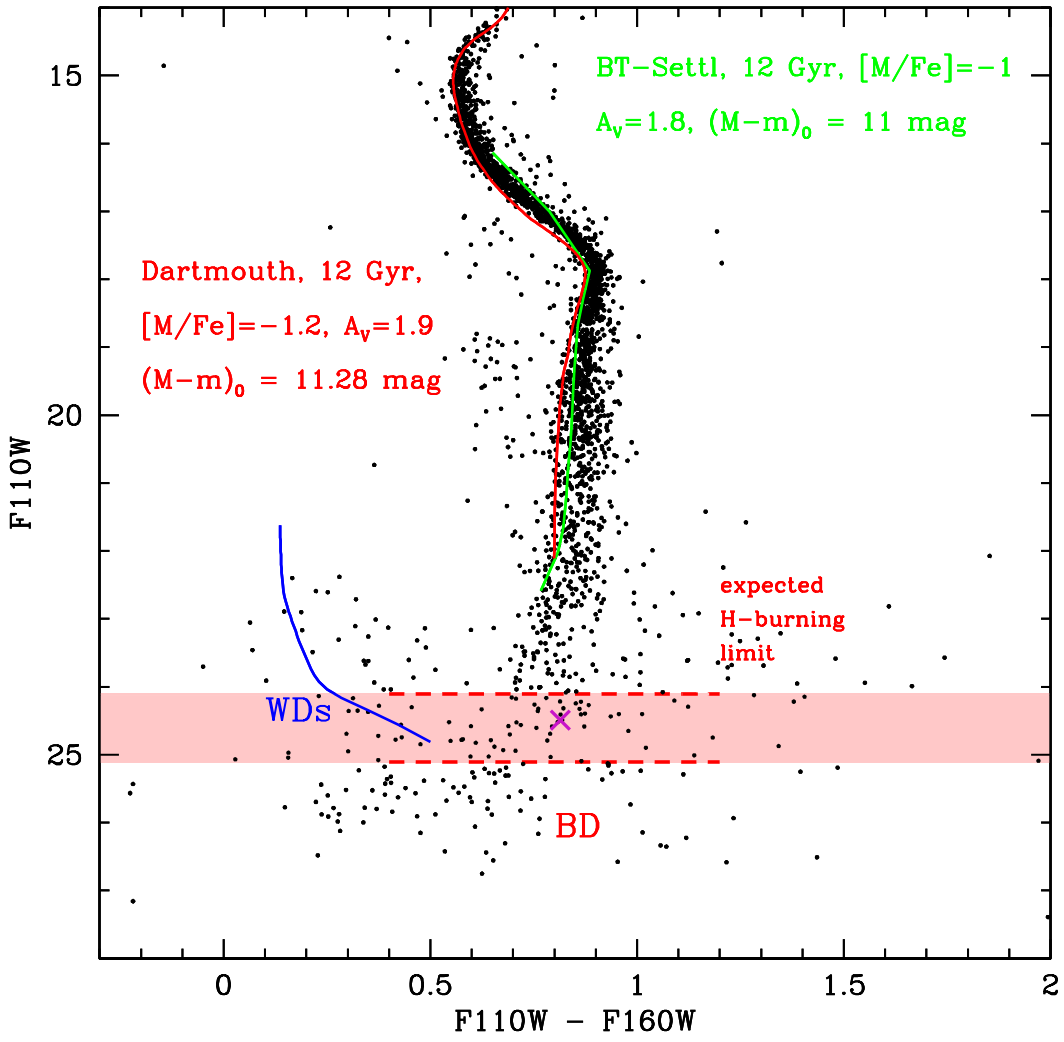

Figure 1: NIR CMD that includes only best-photometry sources. The WD and BD regions have been labeled, and low-mass stellar models (BT-Settl and Dartmouth isochrones) as well as a theoretical WD cooling sequence have been over-plotted. The expected end of the H-burning sequence is marked with red dashed lines and a shaded area. The magenta cross denotes the location of the known field BD SDSS-J125637.13-022452.4 (Burgasser et al. 2009, ApJ, 697, 148), scaled to M4's reddening and distance. Its position in the CMD supports that our data are indeed deep enough to reach well into the BD zone. However, we cannot distinguish between WDs and BDs based on this CMD alone.

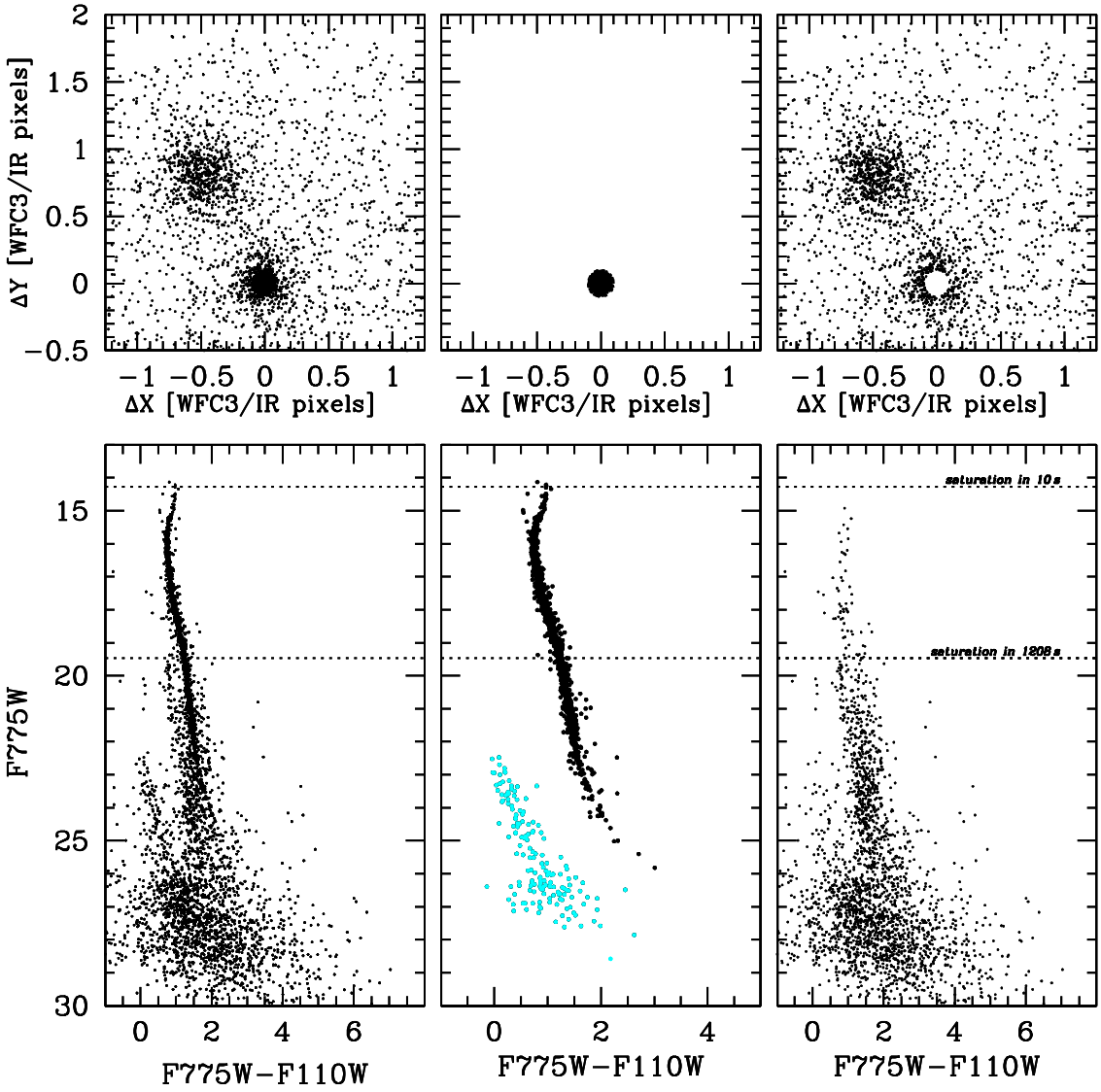

Figure 2: Top row: Vector point diagrams for all NIR sources with optical counterparts with a displacement of no more than 2 WFC3/IR pixels. The corresponding CMDs are plotted in the bottom row: Left: all sources with optical counterparts. Middle: only sources with a displacement of less than 0.1 pixels, suggesting that they are cluster members. Right: remaining field stars. The cluster CMD (middle diagram) is used to select WDs, plotted in light blue.

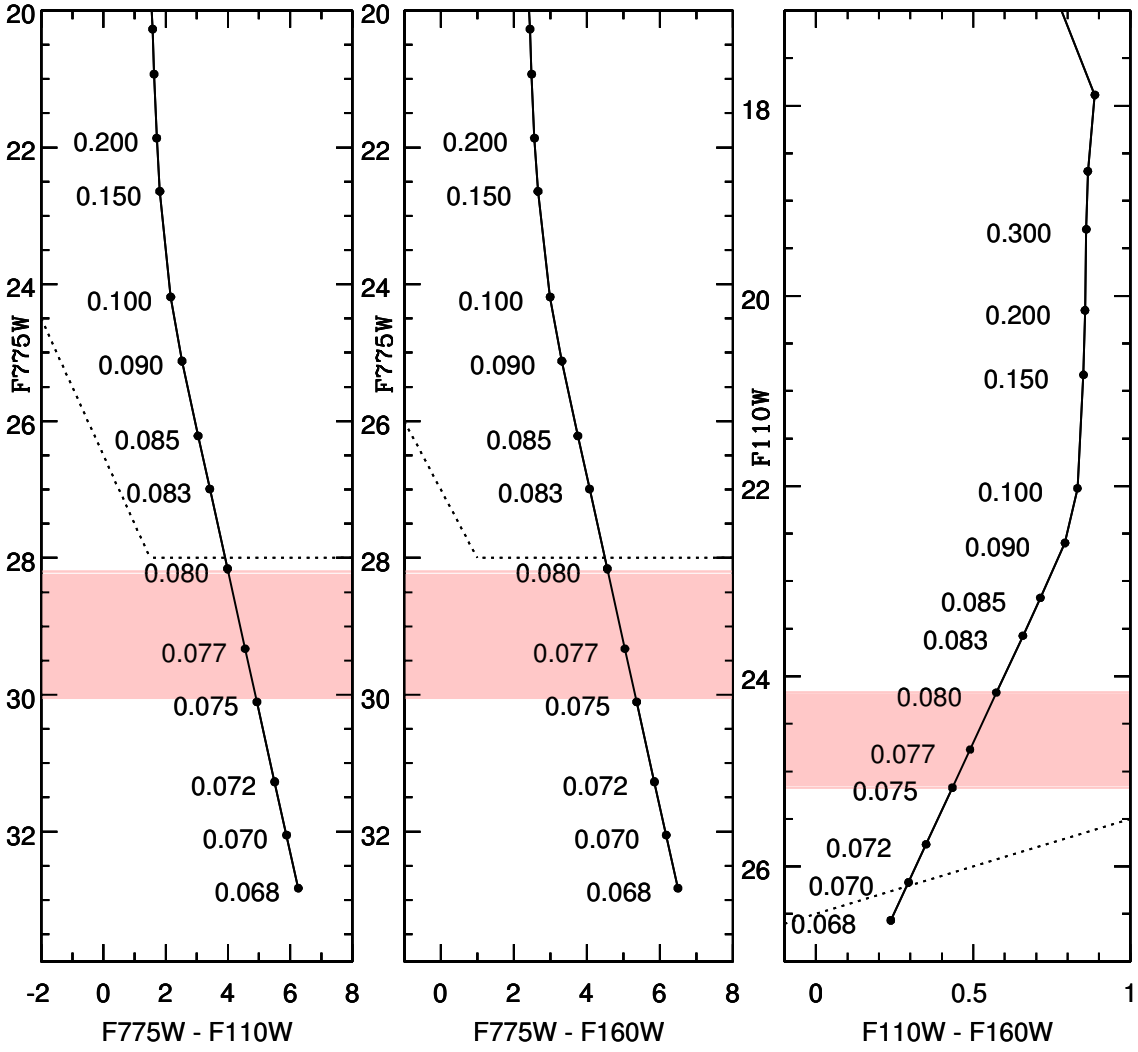

Figure 3: 12 Gyr BT-Settl models in HST/WFC3 filters, scaled to M4's distance, reddening, and metallicity. The models are extrapolated into the substellar regime to 0.068 $M_{\odot}$. Masses are indicated along the sequences. The end of the H-burning sequence is estimated between 0.075 and 0.08 $M_{\odot}$ and is indicated with a light-red shaded area. Detection limits in our NIR and optical data are indicated with dotted lines. We conclude that we have reached beyond the H-burning limit in our NIR CMD and are probably just above or around this limit in our optical-NIR CMDs

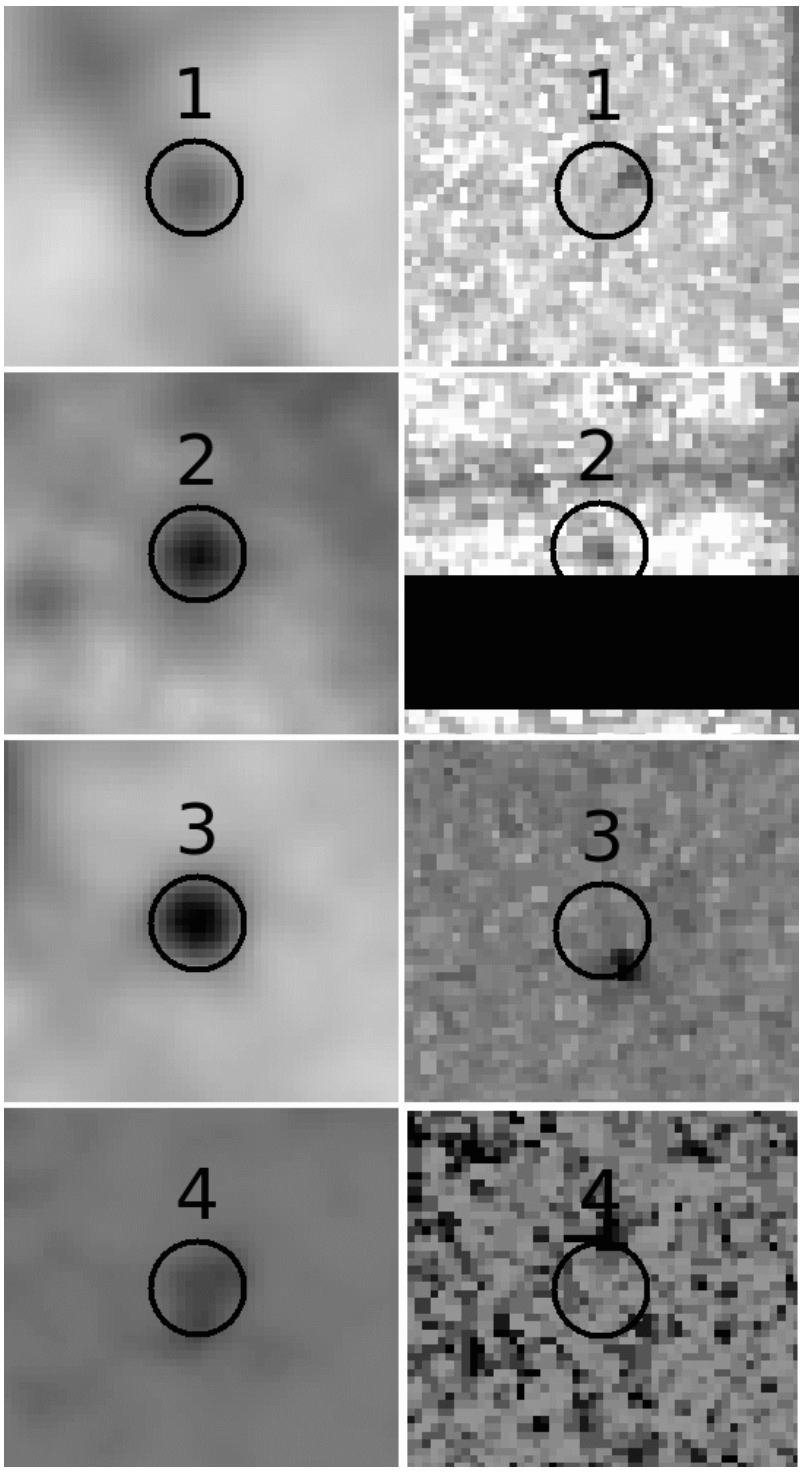

Figure 4: Zoom on the positions of the four BD candidates in the stacked NIR (left) and optical (right) images. The field of view of each image is 1.25" x 1.25" and the radius of the circles is 0.15". North is up and east to the left. As can be seen, all four sources are clear detections in the NIR, but the photometry tools did not return a detection in the optical. We used the optical images to estimate upper optical magnitude limits, which place all four sources in the BD area in all CMDs.

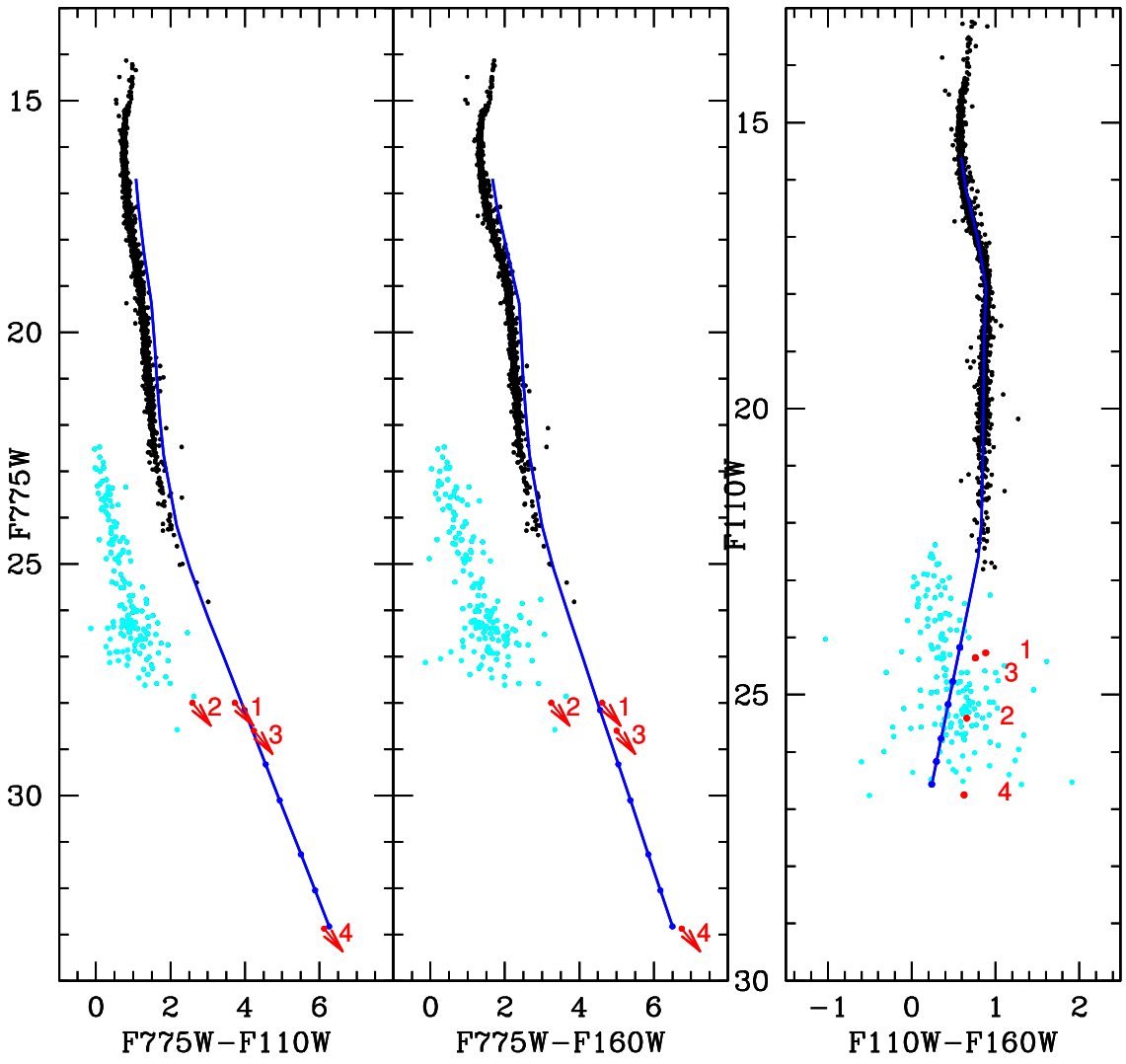

Figure 5: Optical-NIR CMDs (left and middle) and NIR CMD (right) of all sources with an optical counterpart. We also show the position of the four BD candidates, marked with red arrows, assuming the upper optical magnitude limits given in Table 2. We also overplot the extrapolated BT-Settl 12 Gyr isochrone. As can be seen, the position of all four BD candidates is very close to the isochrone, suggesting that they are indeed BDs.

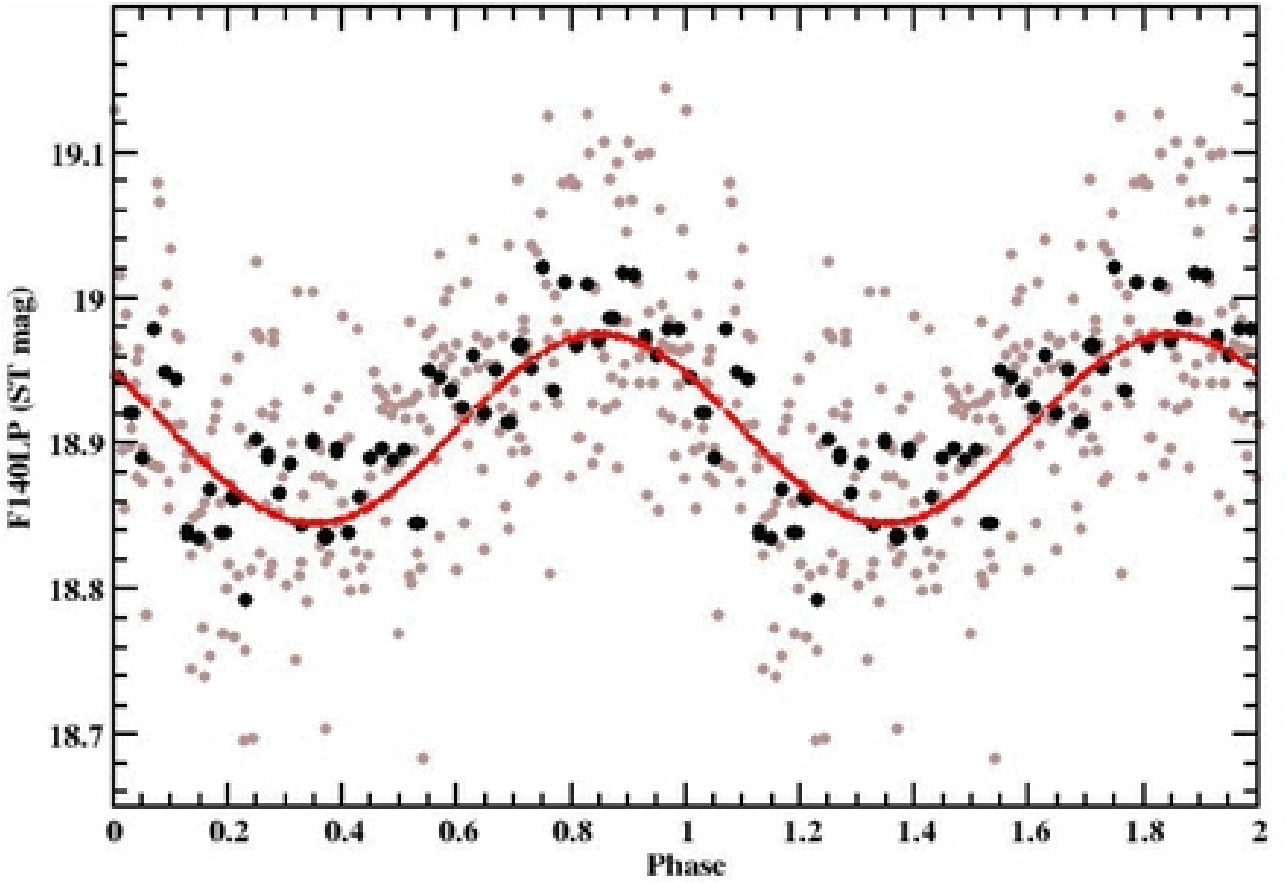

Figure 6: The phased light curve of the FUV variable source in NGC 1851. The data between the phase of 0 and 1 are duplicated between phases 1 and 2. The data have been phased around the 18.05 min period. All 273 individual measurements are plotted as the faint dots. The black solid dots are the average values in phase bins of 0.02. A sine wave with an amplitude of 0.06 mag has been fit to the data to guide the eye.

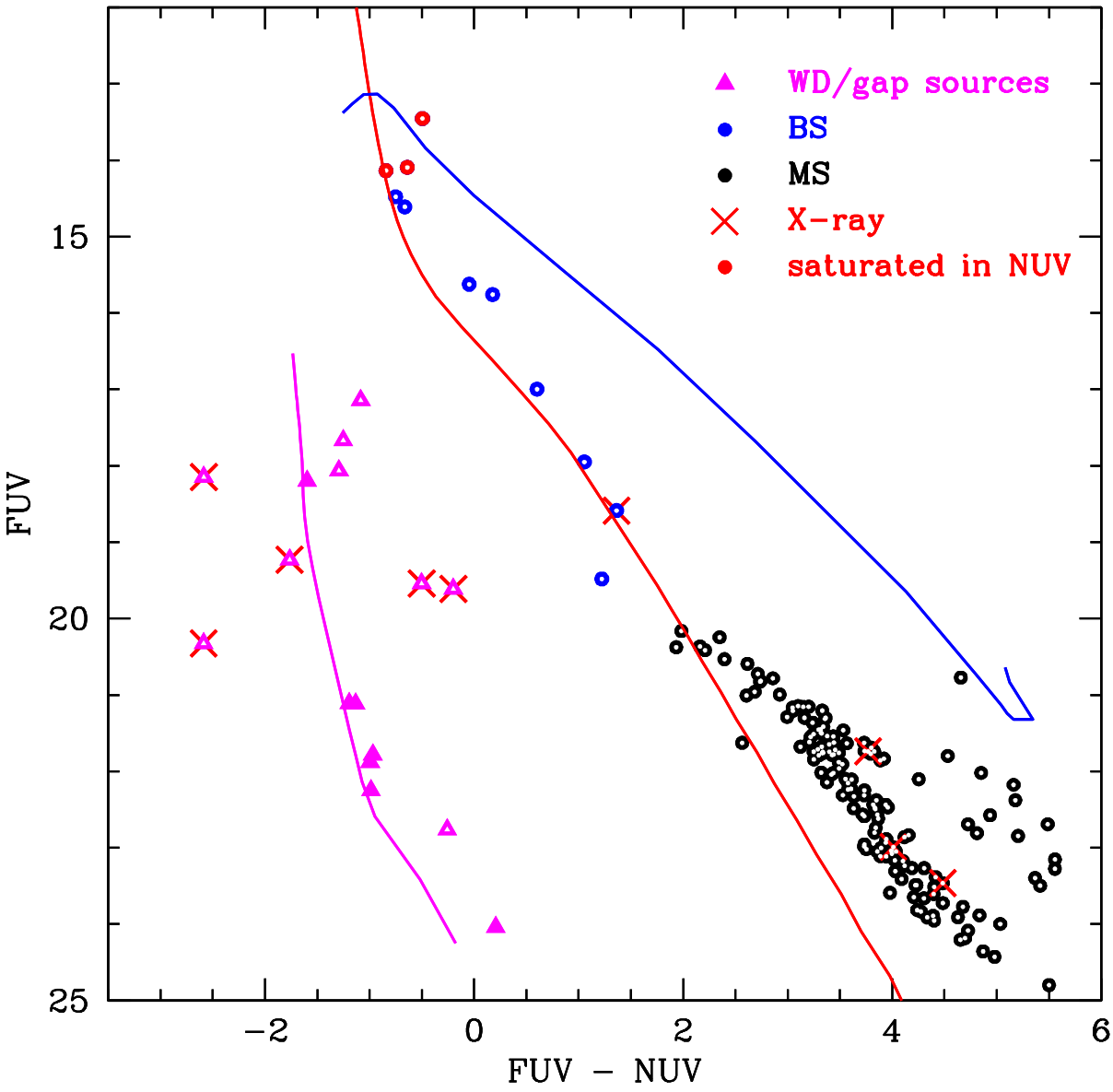

Figure 7: FUV vs. FUV-NUV CMD. For orientation purposes, we also show the synthetic zero-age horizontal branch (blue line, this is the location of the Helium-core-burning stars which then further evolve from here), zero-age main sequence (red line, the location of Hydrogen-burning stars, all stars start their life on this main sequence) and white dwarf cooling sequence (magenta line). Open symbols denote sources with optical counterparts. Large black and blue dots/circles denote main sequence and BS stars, respectively. The three brightest sources are saturated in the NUV and are marked with red circles; their true NUV magnitudes are likely brighter and hence their colour might also be bluer. Sources that have X-ray counterparts are marked with red crosses, and white dwarfs and sources located between the white dwarf cooling and main sequence, which include CVs, are marked with magenta triangles.

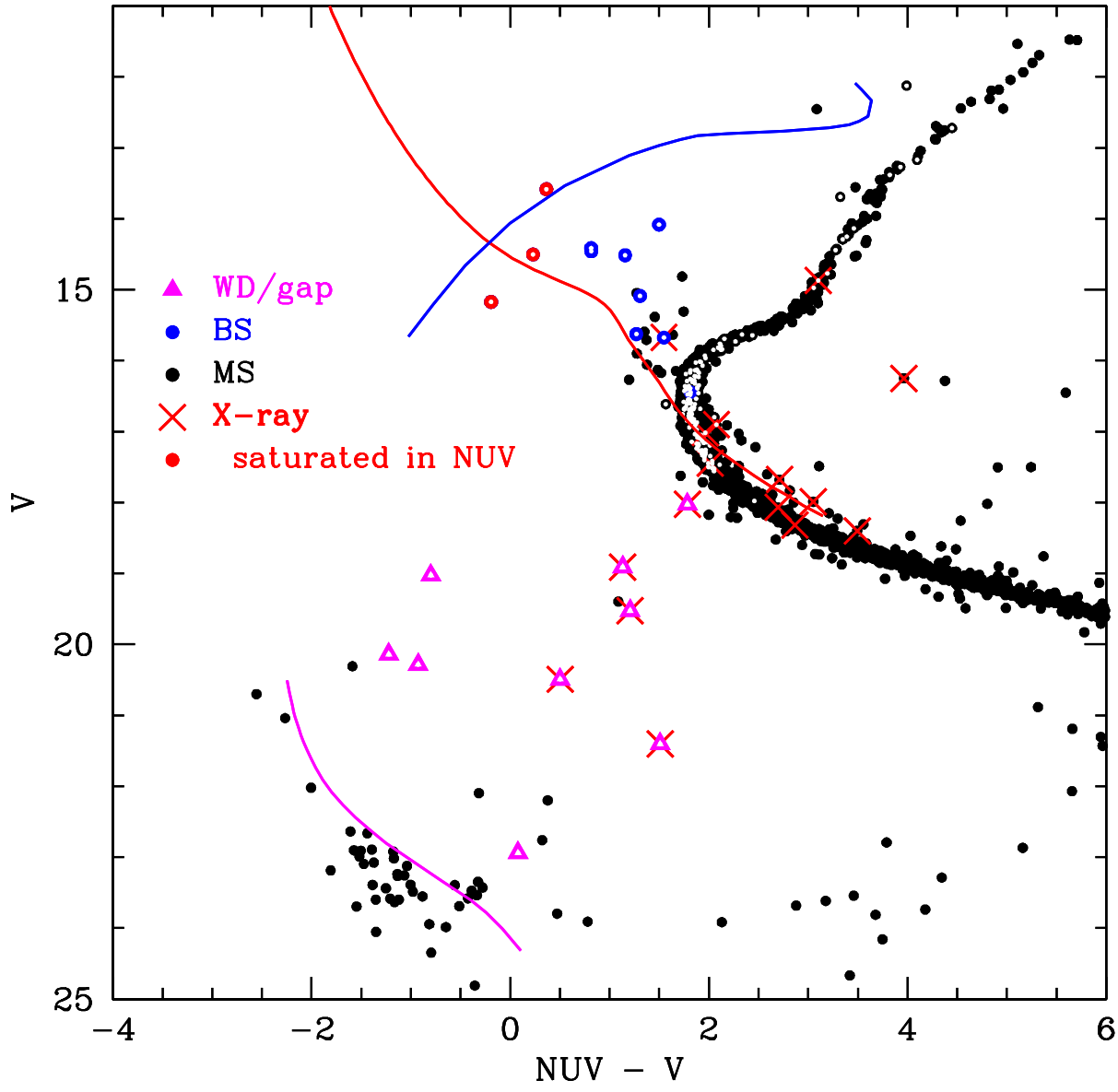

Figure 8: NUV-optical CMD of the cluster NGC 6397. Theoretical tracks have been overplotted to guide the eye and help distinguish the different stellar populations. The symbols and theoretical tracks are the same as in Fig 7. A white dwarf sequence can be clearly seen. Note that this CMD covers a larger area than the FUV images. Sources that have a FUV counterpart are marked with open symbols.

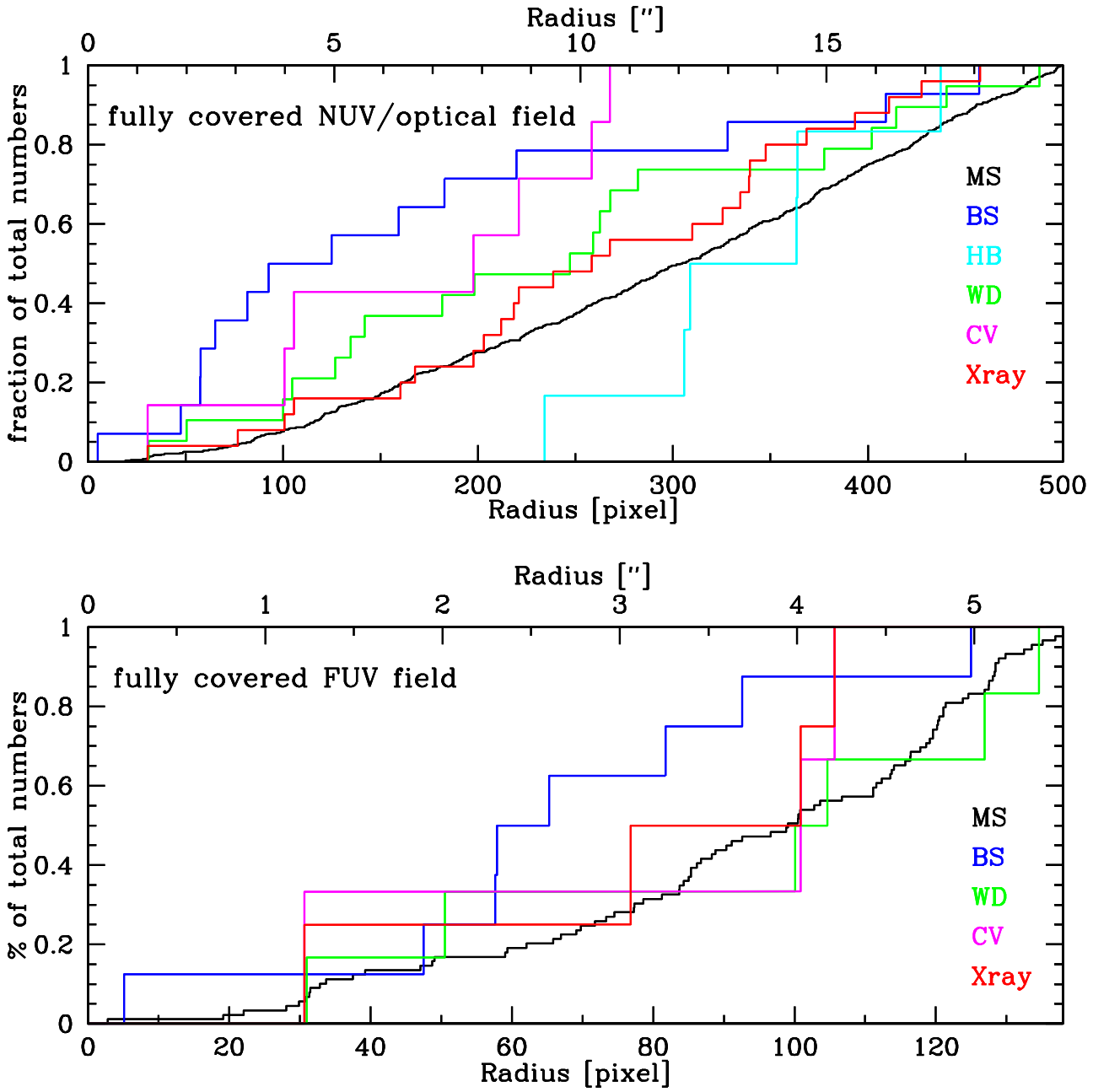

Figure 9: Top panel: Radial distribution of the various stellar population within the inner 19.8" that is fully covered by the NUV and optical data but not the FUV data. Bottom panel: Radial distribution within the inner 5.5" circular area that is fully covered by the FUV master image.

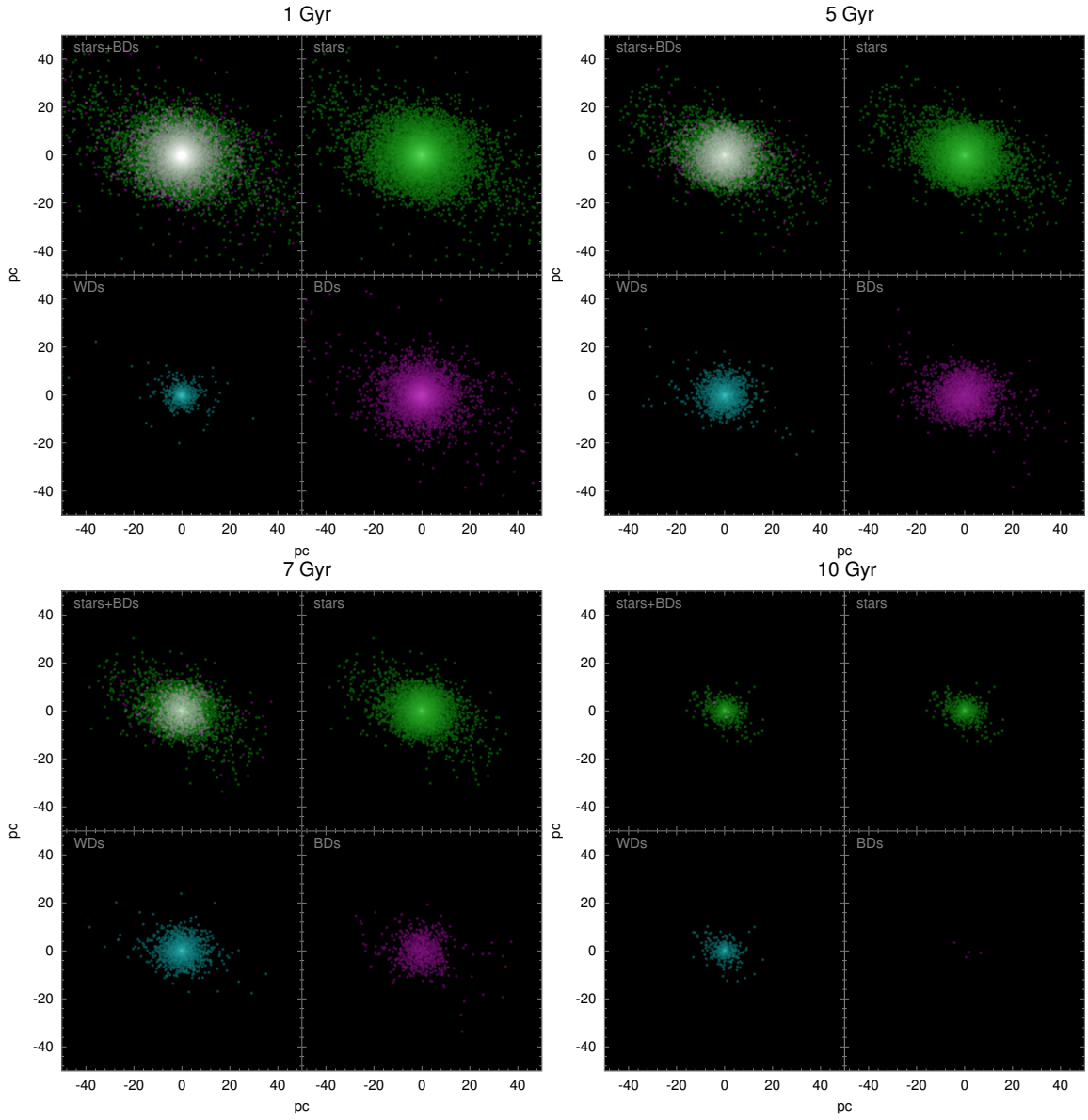

Figure 10: Snapshots of the 100.000 source cluster as it evolves over time. Stars are plotted in green, BDs in red and WDs in blue. After 1 Gyr (top left) the BD distribution follows the distribution of stars. Only few WDs are present, concentrated towards the cluster centre. At 5 Gyr (top, right), the number of WDs has increased, and the number of BDs is decreasing. The cluster is placed in a Galactic tidal field at an orbit corresponding to the GC M4, and the simulations show an elongation of the cluster in the direction of the cluster orbit. After 10 Gyr (bottom right), the cluster has lost nearly 90% of its initial number of sources. WDs largely follow the stellar distribution, whereas only few BDs are left. The simulation also suggests that the very core of the cluster is largely devoid of BDs, so the best place to search for BDs in GCs is not the core region, but also not the very outskirts of the cluster as most BDs will have been ripped away.

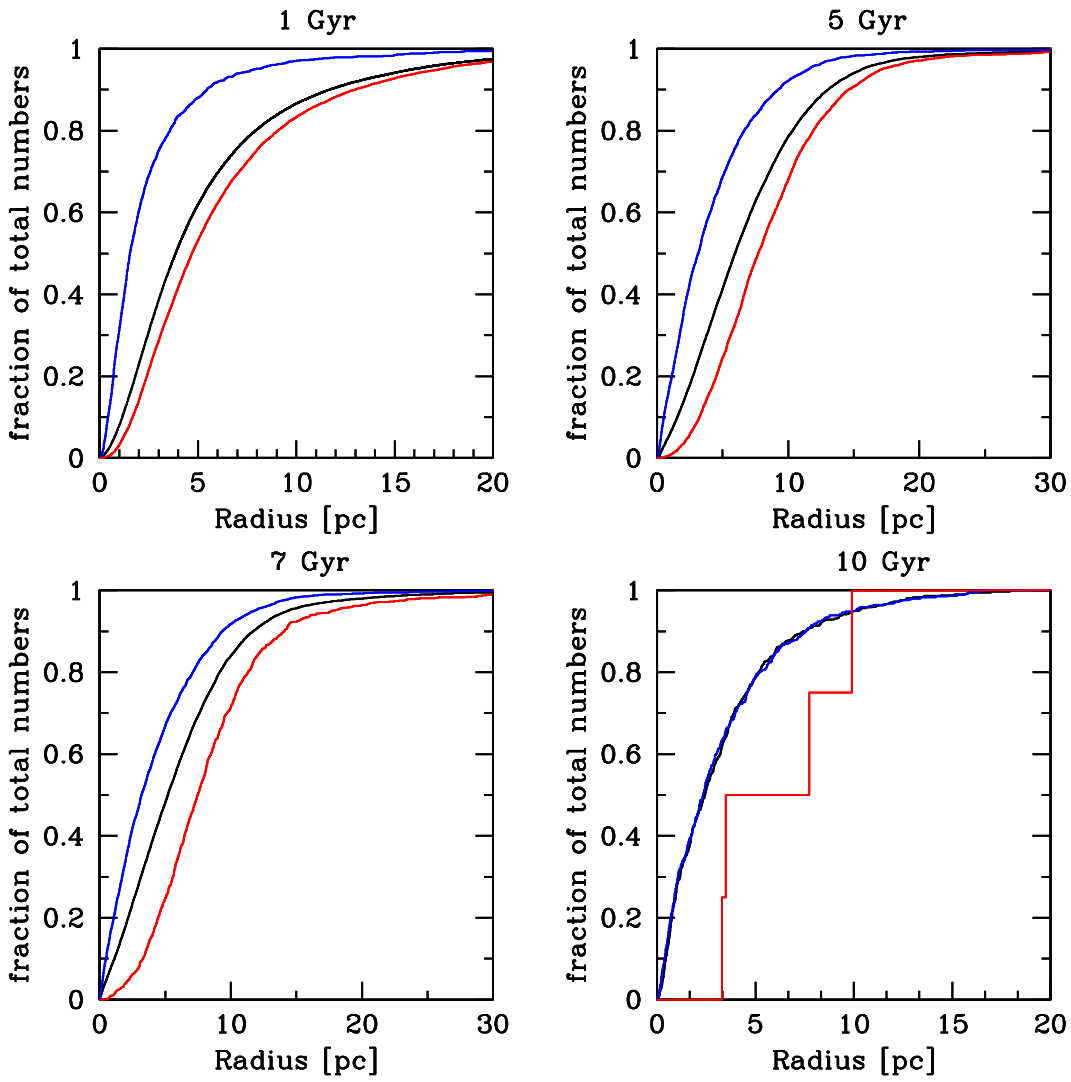

Figure 11: Cumlative radial distribution for the 100.000 bodies simulations. The black line denotes the distribution of all stars, blue of the WDs, and red of the BDs. Towards the end of the simulations, the fractional number of stars left and the fractional number of WDs are nearly identical, with nearly identical distributions, whereas only few BDs are left which are more widely distributed.